DESIGN OPTIMIZATION OF TRANSONIC AIRFOILS

C.-Y. Joh, B. Grossman, and R.T. Haftka

Department of Aerospace and Ocean Engineering
Virginia Polytechnic Institute and State University
Blacksburg, Virginia 24061

N92-13961

ABSTRACT

Numerical optimization procedures have been considered for the design of airfoils in transonic flow based on the transonic small-disturbance (TSD) and Euler equations. A sequential approximation optimization technique was implemented with an accurate approximation of the wave drag based on the Nixon's coordinate straining approach. A modification of the Euler surface boundary conditions was implemented in order to efficiently compute design sensitivities without remeshing the grid. Two effective design procedures producing converged designs in approximately 10 global iterations were developed: interchanging the role of the objective function and constraint and the direct lift maximization with move limits which were fixed absolute values of the design variables.

INTRODUCTION

Current aerodynamic design methods can be broadly categorized as inverse methods, *e.g.*, Volpe and Melnik[1], and numerical optimization methods, *e.g.*, Vanderplaats and Hicks[2]. In general, inverse methods have been widely used as design tools primarily due to their computational efficiency. They do have a weakness associated with the *closure problem*, which generally requires considerable design experience. Also inverse methods, initially developed for potential flows, have been successfully applied to rotational flows based on the Euler equations, *e.g.*, Giles, Drela and Thompkins[3] and the Navier-Stokes equations, *e.g.*, Malone, Narramore and Sankar[4].

Numerical optimization methods have not been widely used in practical airfoil designs primarily due to the large amounts of computational resources needed. Nevertheless, the methods will continue to be developed since they have many advantages such as automated design capability, ability to handle multi-point design and varieties of constraints along with a capability of inclusion into multi-disciplinary design of complete vehicles. A major reason for the large computational effort of numerical optimization methods is the very large number of transonic analyses needed to develop converged designs. Some improvements to the efficiency of numerical optimization methods have been obtained through the implementation of the shape functions, by Vanderplaats and Hicks[2] and Aidala, Davis, and Mason[5], and through the use of efficient optimization procedures, Vanderplaats[6], Joh, Grossman and Haftka[7] and Joh[8].

The motivation for the present work stems from plans to incorporate transonic airfoil designs within an integrated aerodynamic/structural design of an aircraft wing, *e.g.*, Grossman *et al.*[9]. Thus, our objective is to develop efficient numerical optimization procedures for the design of two-dimensional airfoils at transonic speeds, using as few complete transonic analyses as possible.

A preliminary study for this effort is reported in Ref. 7, where some special treatments were developed for design optimization based upon the transonic small-disturbance (TSD) equations. In this paper, we will amplify and improve these ideas and examine in detail the applicability of the methods to the more accurate Euler equation analysis.

DESIGN FORMULATION

Design Problem

The design problem considered can be stated as:

$$\text{maximize} \quad C_l(\bar{X})$$
$$\text{such that} \quad C_d(\bar{X}) \leq C_{d_i}, \tag{1}$$
$$A(\bar{X}) \geq A_{min},$$

where $\bar{X}$ is the vector of design parameters $\bar{X} = (X_1, X_2, \ldots, X_N)^T$ specifying the airfoil geometry, C_d is the drag coefficient due to wave drag, C_{d_i} is the prescribed upper limit on wave drag, A is

ANALYTICAL FORMULATION

TSD Analysis

The first approach taken is based on a TSD formulation. This approach is based on an asymptotic expansion of the perturbation potential in the limits of airfoil thickness $(t/c) \rightarrow 0$ and free-stream Mach number $M_\infty \rightarrow 1$, e.g., Ref. 12. The governing equation may be written as

$$\left[(1 - M_\infty^2)\phi_x - \frac{(\gamma+1)}{2} M_\infty^2 \phi_x^2 \right]_x + \phi_{yy} = 0, \tag{3}$$

with the surface boundary condition on the airfoil surface, $y = Y(x)$ expanded to be

$$\frac{\partial \phi}{\partial y}(x, 0) = \frac{dY}{dx}, \qquad 0 \le x/c \le 1. \tag{4}$$

It may be noted that the governing equation retains the important non-linear effects of transonic flows but does not include the effects of entropy change across shock waves. Also, since the airfoil surface boundary condition is applied along the axis and not on the actual surface of the airfoil, the calculation can be performed on a simple Cartesian grid. This is useful in the design problem, since we can efficiently utilize a fixed grid even with changing airfoil geometries. The specific analysis code used for our TSD calculations is TSFOIL described in Ref. 13.

Euler Analysis

In order to evaluate whether the design procedures developed using the approximate TSD analysis are valid for more accurate flow field methods, we have investigated the airfoil design with the Euler equations. We utilize the complete set of governing equations for an inviscid, non-heat conducting, adiabatic flow with negligible body forces. The equations may be written in conservation-law form in Cartesian coordinates as

$$\frac{\partial Q}{\partial t} + \frac{\partial F}{\partial x} + \frac{\partial G}{\partial y} = 0, \tag{5}$$

where

$$Q = \begin{pmatrix} \rho \\ \rho u \\ \rho v \\ \rho e_0 \end{pmatrix}, \quad F = \begin{pmatrix} \rho u \\ \rho u^2 + p \\ \rho uv \\ (\rho e_0 + p)u \end{pmatrix}, \quad G = \begin{pmatrix} \rho v \\ \rho uv \\ \rho v^2 + p \\ (\rho e_0 + p)v \end{pmatrix}, \tag{6}$$

with velocity components u, v, density ρ, total energy per unit mass $e_0 = e + (u^2 + v^2)/2$, with e being the internal energy per unit mass and pressure p, which for a perfect gas may be expressed as $p = (\gamma - 1)[\rho e_0 - \rho(u^2 + v^2)/2]$. The surface boundary conditions for the Euler equations, representing no flow through the solid surface may be expressed as

$$v(x, Y) = Y'(x)u(x, Y), \qquad 0 \le x/c \le 1, \tag{7}$$

where a prime denotes differentiation with respect to x. Thus we see that the boundary conditions must be applied on the actual airfoil geometry, requiring a new mesh to be generated at each stage of the design process. We partially alleviate the computational burden of re-creating the grid for each geometry by assuming that design changes proceed slowly, and for a specified number of cycles consider the grid to be fixed to a baseline airfoil geometry. Then the surface boundary condition must be altered to allow a small amount of mass transpiration through the surface to approximately account for the changing geometry. This procedure fits in well with the sequential approximate optimization algorithm used in the design process, which imposes move limits on the design. For each optimization cycle a baseline geometry will define the grid and the grid will be kept fixed throughout the approximate optimization cycle. This greatly reduces the computational effort for the Euler designs.

Let the subscript b refer to the body surface of the new airfoil and the subscript b_0 refer to the body surface of the baseline airfoil. The exact surface boundary condition on the new airfoil surface is the vanishing of the normal velocity $\vec{V}_b \cdot \hat{n}_b = 0$ or, as in Eq. (7)

$$v_b = Y'u_b. \tag{8}$$

the airfoil cross-sectional area, non-dimensionalized by c^2, with c the airfoil chord and A_{min} is the minimum required area. The design is performed at a free-stream Mach number of $M_\infty = 0.75$ and zero angle of attack, $\alpha = 0$.

This type of problem has been solved first by Vanderplaats and Hicks[2] with a full potential code, requiring 70 exact analyses. In Ref. 6, the same problem required 44 exact analyses with a sequential optimization technique and data base approach where all the previous design information is stored and reused for constructing higher-order approximations.

Here, we will examine the effects of utilizing two different codes, one a more approximate transonic small-disturbance (TSD) analysis and the second, a more exact inviscid Euler analysis. However, due to the different approximations in the two analyses, particularly the neglect of entropy jumps across the shock waves, the wave drag values are found to be different, with the TSD result at a lower level. In order to develop somewhat similar designs between the Euler and TSD methods it was found necessary to utilize a larger value of C_{d_t} in Eq. (1) for the Euler designs.

Shape functions and Design Variables

We have chosen to design the airfoil using shape functions following the successful implementation of Vanderplaats and Hicks[2];

$$Y = \sum_{i=1}^{N+2} X_i Y_i \left(\frac{x}{c}\right),$$

(2)

where $Y \equiv y/c$ with y being the airfoil ordinate and c the airfoil chord length. The specified shape functions Y_i are functions of the non-dimensional abscissa x/c and the parameters X_i are the design variables. For the shape functions here, we selected four existing airfoils $(N = 4)$, namely, $NACA\ 2412, NACA\ 64_1 - 412, NACA\ 65_2 - 415$ and $NACA\ 64_2A215$. There are two additional shape functions for imposing the boundary conditions at the trailing edge of the airfoil. These are $Y_{N+1} = +x/c$ on the upper surface and zero on the lower surface, and $Y_{N+2} = -x/c$ on the lower surface and zero on the upper surface. Usually with TSD analyses an open trailing edge is considered; here we specify this thickness to be .0025c. For Euler analyses a closed trailing edge is utilized. This fixes the values of the coefficients X_{N+1} and X_{N+2} in terms of $X_1, \ldots, X_N$.

Approximate Optimization

When a design optimization is coupled with expensive numerical analysis code, most of the cost of the optimization is associated with the exact analyses and sensitivity calculations. Even with the most efficient transonic flow analysis code, the cost of the design process may be prohibitive if the analysis code and an optimization algorithm are linked together directly, so that full analyses are made for all the function evaluations during the design process. Instead we utilize a sequential approximate optimization algorithm[10]. This approach replaces the original objective function and constraints with approximations based upon nominal values and derivatives at an initial point. Additionally, move limits are used to prevent the design from moving outside the bound of validity of the approximations. Each approximate optimization problem is solved until an optimum is found, and then a new approximation is constructed there, and the design optimization process is repeated until convergence is achieved. An approximate optimization is typically referred to as an optimization cycle, and this is also the terminology used here. A key part of implementing a sequential approximation algorithm involves the approximation of the objective function and constraints. We have found that these approximations play a crucial role in the design process. The procedures that we have developed for approximating the lift and drag appear in detail later in this paper.

The specific optimizer used for our study is the general purpose optimization program NEW-SUMT-A[11] which is based on a quadratic extended interior penalty function and Newton method for unconstrained minimization. The program provides the user with several approximation-switching and move limit strategies.

Now we utilize the grid system which was generated for the baseline airfoil to analyze the flow over the new airfoil. Thus it is necessary to evaluate the new normal and tangential velocities on the baseline airfoil surface Y_0. (The normal velocity on the baseline airfoil $\vec{V}_{b_0} \cdot \hat{n}_{b_0}$ will not be zero). This can be achieved by expanding the Cartesian velocity components at the baseline airfoil surface in terms of the coordinates of the new airfoil surface as

$$v_{b_0} = v_b + (\frac{\partial v}{\partial y})_b (Y - Y_0) + \ldots = v_b + \mathcal{O}(\Delta Y), \tag{9.a}$$

$$u_{b_0} = u_b + (\frac{\partial u}{\partial y})_b (Y - Y_0) + \ldots = u_b + \mathcal{O}(\Delta Y), \tag{9.b}$$

where $\Delta Y = Y - Y_0$. Thus using the boundary condition (8) we have $v_{b_0} = u_b Y' + \mathcal{O}(\Delta Y)$ and $u_{b_0} = u_b + \mathcal{O}(\Delta Y)$. We can write these in terms of normal and tangential velocity components to the baseline geometry as

$$V_{n_{b_0}} = \frac{v_{b_0} - u_{b_0} Y_0'}{\sqrt{1 + Y_0'^2}}, \tag{10}$$

$$V_{t_{b_0}} = \frac{u_{b_0} - v_{b_0} Y_0'}{\sqrt{1 + Y_0'^2}}. \tag{11}$$

Using Eqs. (8)–(11), we can write an expression for $V_{n_{b_0}}$ in terms of $V_{t_{b_0}}$ which takes into account the vanishing of the normal velocity at the new airfoil surface, $V_{n_b} = 0$, as

$$V_{n_{b_0}} = \frac{V_{t_{b_0}}}{1 + Y'Y_0'} (Y' - Y_0'), \tag{12}$$

where terms of $\mathcal{O}(\Delta Y)$ have been neglected.

The boundary conditions for the Euler calculation may be evaluated by extrapolating from the field points to the surface $y = Y_0$ values of ρ_{b_0}, p_{b_0} and u_{b_0} and v_{b_0}. The tangential velocity $V_{t_{b_0}}$ is computed from Eq. (11) and the normal velocity $V_{n_{b_0}}$ from Eq. (12). Values of the total energy are computed from

$$(\rho e_0)_{b_0} = \left[\frac{p_{b_0}}{\gamma - 1} + \frac{\rho_{b_0}(V_{n_{b_0}}^2 + V_{t_{b_0}}^2)}{2} \right]. \tag{13}$$

The specific analysis code used for our Euler calculations is FLOMG which is based on Jameson's time-stepping[14] and multigrid algorithms[15]. Although the code was developed by Swanson and Turkel[16] for solving the Navier-Stokes equations, we will utilize it only in the inviscid, Euler solver mode.

LIFT AND DRAG APPROXIMATIONS

We first considered simple linear approximations for the lift and wave drag, as:

$$f = f^0 + \sum_{i=1}^{4} \frac{\partial f}{\partial X_i} (X_i - X_i^0), \tag{14}$$

where f is either the lift or the wave drag and f^0 is evaluated with the initial design parameters $X_1^0, \ldots, X_4^0$. The sensitivity derivatives, $\partial f / \partial X_i$ are evaluated using one-sided finite-difference expressions. The effectiveness of the lift approximation is indicated in Tables 1a and 1b for both TSD and Euler analysis methods. We see that when the design variables are changed by as much as 2%, the linear approximation of the lift coefficient remains within a 2% accuracy, compared to the exact analysis, for the TSD solutions and to within 0.5% for the Euler solutions. However, this situation is not repeated for the drag approximation. As seen in Tables 1a and 1b the linear approximation for the wave drag does not correlate closely with the exact results, with errors of 25% for the TSD solutions and 15% for the Euler solutions, when the design variables change by 2%. This result

was not unexpected since transonic flows are very nonlinear and shock-wave movement must play an important role in the wave-drag approximation.

In order to better approximate the wave drag, we considered the method of strained coordinates for perturbations of transonic flows with shock waves, introduced by Nixon[17]. This method has been applied for airfoil approximations by Stahara[18]. In this method, the perturbations are made in a *strained* coordinated system where the shock remains fixed. Coordinate straining uses the axial position of the shock wave on the airfoil, x_s and the height of the tip of the shock wave above the airfoil, y_t. When x_s changes by Δx_s and y_t changes by Δy_t, the coordinates (x, y) of each point in the flow field are changed by Δx and Δy given by

$$\Delta x = s(x)\,\Delta x_s, \qquad \Delta y = \frac{y}{y_t}\,\Delta y_t. \tag{15a,b}$$

For the TSD analysis, following Ref. 17, the straining function $s(x)$ is taken as

$$s(x) = \frac{x(c - x)}{x_s(c - x_s)}, \tag{16}$$

which is valid for $0 \le x \le c$ and is equal to zero otherwise.

For the TSD analysis, the strained coordinates are used first in the process of calculating finite-difference sensitivity derivatives according to the following steps:

1. The i-th design variable is perturbed by ΔX_i and the corresponding Δx_s and Δy_t are calculated from a new solution of the flow field and used to approximate the shock sensitivities

$$\frac{\partial x_s}{\partial X_i} \simeq \frac{\Delta x_s}{\Delta X_i}, \qquad \frac{\partial y_t}{\partial X_i} \simeq \frac{\Delta y_t}{\Delta X_i}. \tag{17a,b}$$

2. The flow-field sensitivities are approximated, using Δx and Δy from Eqs. (15a,b), in terms of the axial velocity for the nominal design u^0 and the axial velocity for the perturbed flow field u as

$$\frac{\partial u}{\partial X_i}(x, y) = \frac{1}{\Delta X_i}[u(x + \Delta x, y + \Delta y) - u^0(x, y)]. \tag{18}$$

The strained coordinates are used again in approximating the flow at a new design point $\bar{X}$ as follows: First the new shock location and shock-tip position are calculated by a linear approximation

$$\Delta x_s = \sum_{i=1}^{4} \frac{\partial x_s}{\partial X_i}(X_i - X_i^0), \qquad \Delta y_t = \sum_{i=1}^{4} \frac{\partial y_t}{\partial X_i}(X_i - X_i^0). \tag{19a,b}$$

Values of Δx and Δy are calculated from Eqs. (15a,b) and then the axial velocity u is estimated from

$$u(x + \Delta x, y + \Delta y) = u^0(x, y) + \sum_{i=1}^{4} \frac{\partial u(x, y)}{\partial X_i}(X_i - X_i^0). \tag{20}$$

The wave drag coefficient is determined from a contour integral of the jump in pressure across the shock, which may be written as[13]:

$$C_d = -\delta^{5/3} M_\infty^{-3/4} \frac{(\gamma + 1)}{\gamma} \int_{shock} [u]^3\, dy, \tag{21}$$

where M_∞ is the free-stream Mach number, δ is the nominal airfoil thickness, γ is the ratio of specific heats and $[u]$ is the *jump* in u across the shock.

For the Euler analysis a different implementation of the method of the strained coordinates is utilized. First, since the wave drag is calculated by integrating surface pressures, only the solution at the body surface needs to be approximated. The coordinate straining in y direction is not necessary. Furthermore, accurate solutions for the Euler wave drag were obtained by approximating the surface

pressures directly, rather than computing from the flow field. Thus the surface pressure sensitivity and approximation, respectively were calculated as

$$\frac{\partial p}{\partial X_i}[x, Y_0(x)] = \frac{1}{\Delta X_i}\left(p[x + \Delta x, Y_0(x + \Delta x)] - p^0[x, Y_0(x)]\right), \tag{22}$$

$$p[x + \Delta x, Y_0(x + \Delta x)] = p^0[x, Y_0(x)] + \sum_{i=1}^{4} \frac{\partial p[x, Y_0(x)]}{\partial X_i}(X_i - X_i^0), \tag{23}$$

where Δx is the amount of coordinate straining and the superscript 0 corresponds to the value for the nominal design. The pressure on the perturbed geometry can be approximated by using Taylor series expansion about this pressure on the baseline geometry and then the wave drag coefficient is determined from the integration of the approximate surface pressure force in x-direction.

The non-uniqueness of the straining function has been discussed in Refs. 17 and 18. Here, several tests were made to select the best straining function in terms of approximation accuracy for the Euler analysis. The linear piecewise continuous straining appeared to be most accurate and well-behaved. This has been also pointed out with the full potential method in Ref. 18. The linear piecewise continuous function is given by

$$s(x) = \begin{cases} x/x_s & ; 0 \le x \le x_s, \\ (c - x)/(c - x_s) & ; x_s \le x \le c, \end{cases} \tag{24}$$

was used, where x_s is the location of shock wave.

The results of Nixon's coordinate-straining approximation on the drag coefficient are tabulated in Tables 1a and 1b. It is seen to significantly improve the wave drag approximation, with the errors reducing to less than 3% for the TSD solutions and 7% for the Euler solutions, when the design variables change by 2%. The effect of this approximation on the airfoil pressure distributions is shown in Figs. 1a and 1b.

DESIGN RESULTS

In this section we consider several optimization strategies for the transonic airfoil design problem of maximizing lift with constraints on wave-drag and airfoil cross-sectional area as given by Eq. (1). The minimum non-dimensional area is taken to be $A_{min} = 0.075$. The wave drag constraint is taken to be $C_{d_t} = 0.004$ for the TSD designs and $C_{d_t} = 0.010$ for the Euler designs.

Designs based on the TSD analysis

Strategy A: Approximate Optimization with Tight Move Limits - The first optimization strategy that we employed consisted of imposing tight move limits in the approximate optimization procedure. The results of applying this strategy with two different initial designs are tabulated in Tables 2a and 2b. In the first case, we imposed 5% move limits in order to keep the error in the drag approximation to within 10%. The solution ceased to improve after 27 iterations and the move limits were tightened to 2.5%. At 60 iterations the move limits were further reduced to 1.25% and the solution was considered to be converged. However, in the second case, corresponding to different initial conditions, employing a similar strategy resulted in a completely different design, as can be seen in Table 2b.

In order to examine whether these solutions were local maxima we considered the following: denoting the first converged solution as $\bar{X}^1$ and the second as $\bar{X}^2$, we defined an intermediate design state

$$\bar{X} = \bar{X}^2 + \xi(\bar{X}^1 - \bar{X}^2), \tag{25}$$

where the parameter ξ may be considered the proportional distance of the intermediate design between $\bar{X}^2$ and $\bar{X}^1$. We computed both approximate and exact value for the lift and wave-drag coefficients for intermediate designs with $0 \le \xi \le 1$. The results are plotted in Fig. 2. From the upper chart in Fig. 2 we see that the lift coefficient is well-behaved between design state 2 and state 1, exhibiting no local maxima or minima. In the lower chart, we see that the culprit is the drag-coefficient constraint, which exhibits a very *wavy* behavior about $C_d = 0.0040$. Thus we can see that if we are a design state 2, the optimizer would prevent you from moving toward state 1, since that would be a direction of increasing drag.

Strategy B: Drag Minimization followed by Lift Maximization - The strategy that we found to be useful to avoid the problems associated with the drag constraint consisted of interchanging the role of the drag constraint with the lift objective function: We had noticed that design problems of minimizing drag with a constraint on the lift were well behaved. In order to solve the design problem formulated in this paper, we adopted the following strategy: first the wave-drag coefficient was minimized with a constraint on the lift coefficient of $C_l \geq 0.5$ and cross-sectional area ratio $A \geq 0.075$; then, when C_d was below 0.004 we reverted back to the original design formulation of maximizing C_l with constraints of $C_d \leq 0.004$ and $A \geq 0.075$.

The results of this strategy were very good. We found that during the drag minimization phase, very large move limits, as large as 500% could be used without any adverse effects. During the lift maximization phase, move limits of 20% were imposed. This strategy seemed to be robust, and the solutions did not depend upon the initial data. The design history for the first case, starting from $\bar{X}^0 = (1.0, \ 0.0, \ 0.0, \ 0.0)^T$ is tabulated in Table 3a. The design results for four different initial designs are summarized in Table 3b. In all cases convergence to nearly the same design result was obtained in 8–13 design cycles. The pressure coefficient and corresponding airfoil shape of the initial and final designs tabulated in Table 3a, are shown in Fig. 3. The design appears to be physically reasonable, with a weakened shock wave and lift increased through aft camber.

Strategy C: Approximate Optimization with Absolute Move Limits - After we obtained successful design results using the strategy B, we carefully investigated the TSD solutions to determine the cause of the noisy drag calculation. We found that the spline interpolation routine in the TSFOIL program generated an irregular airfoil leading-edge geometry. Although this should not be important in the TSD solutions, which lose their validity at the leading edge, it clearly affected wave drag calculations and generated noise. We replaced the original routine with a more effective interpolation based on the approximate arc-length of the airfoil with a periodic boundary condition and consequently was able to generate fairly smooth and round noses.

Next, we attempted to directly maximize the lift with tight move limits using the new geometry interpolations. The design process behaved much better due to the considerably reduced noise in the wave drag, even though the noise was not removed completely. We felt that we should increase the move limits in order to get faster convergence. We also found that we could produce reasonably efficient designs using move limits which were fixed absolute values rather than percentages of the design variables. By several tests, we found that initially 0.5 could be used without any adverse effect and then it was reduced by half when the design did not make any improvement. The design results using this procedure are tabulated in Tables 4a and 4b. We experienced some convergence difficulties with TSFOIL using this approach. We will examine this strategy in more detail with the Euler analysis method.

For the TSD designs, each exact airfoil analysis using the program TSFOIL required 10–15 CPU seconds on the IBM 3090 at V. P. I. & S. U., with N+1(5) analyses needed per design cycle. The approximate optimization using the program NEWSUMT-A required 10–12 CPU seconds on the same computer.

Designs based on the Euler analysis

On the basis of the TSD design experience, we applied the two successful design strategies, B and C to the same design problem with the Euler analysis. Recall that the wave-drag constraint value was changed to 0.01 for the Euler design due to the differences in wave drag prediction between the TSD and Euler methods. The original value of 0.004 was found to be too stringent for the design problem with the Euler analysis.

Strategy B: Drag Minimization followed by Lift Maximization - Table 5a represents the complete design history for the first case, starting from $\bar{X}^0 = (1.0, \ 0.0, \ 0.0, \ 0.0)^T$. In the lift maximization phase, initially 50% move limits were utilized, which yielded a large improvement in the lift coefficient to a value of $C_l = 0.7136$ for the first 8 iterations. After that we reduced move limits by half twice and then finally we imposed very tight move limits of 2% which after 25 iterations resulted in $C_l = 0.7144$. For the purposes of this study, we consider the design achieved after 8 iterations, corresponding to the 50% move limits to be acceptable as a final design. The equivalent value of C_l in the table is the relevant estimated lift coefficient when all of the violated constraints are brought to be critical.

Lagrange multipliers are used to estimate these equivalent lift coefficients since they represent the amount of change in the objective function due to the unit change in a constraint at an optimum. This provides us information whether the design makes true improvement or not. We found that this strategy was as robust and efficient for the design based on the Euler method as it was for the TSD method. As shown in Table 5b, four different initial conditions yielded nearly the same final design in 10–12 design cycles. The pressure distributions and corresponding airfoil shapes of the initial and final designs are shown in Fig. 4.

Strategy C: Lift Maximization with Absolute Move Limits - The complete design history for the first case with strategy C is tabulated in Table 6a. Here also, we consider the design achieved after 9 iterations, corresponding to the 0.5 move limits to be acceptable as a final design. Table 6b represents the summary of the design results for four different cases. All cases did converge to approximately the same design result in 8–10 global iterations.

For the Euler designs, each exact airfoil analysis using the program FLOMG required approximately 40 CPU seconds on the CRAY 2S at NASA Langley. The approximate optimization using the program NEWSUMT-A required 40–60 CPU seconds on the IBM 3090 at V. P. I. & S. U. The additional computer time associated with the approximate optimization of the Euler design is partly related to the more complicated wave drag calculation compared to that used for the TSD design.

Error Magnification during Optimization

Table 7 compares the lift/wave drag ratios predicted by TSD and Euler methods for the four airfoils used in the shape definition and the optimum TSD airfoil. It is seen that the agreement between TSD and Euler is much poorer for the optimized airfoil. This indicates that there may be a risk associated with optimization based on an approximate method. The optimization procedure may "improve" the design by exploiting the weaknesses of the approximation.

CONCLUSIONS

We have considered numerical optimization procedures for the design of transonic airfoils based on the transonic small-disturbance (TSD) and Euler equations. A sequential approximate optimization procedure was implemented with accurate approximation of the wave drag based on the Nixon's coordinate straining technique. A modification of the surface boundary conditions was utilized in order to efficiently compute sensitivity derivatives without remeshing the grid with the Euler analysis.

The airfoil design problem which we considered consisted of maximizing the lift with constraints on the wave drag and area. We found that when the computed drag did not vary smoothly with the design parameters, the optimization process produced local extrema. A procedure interchanging the role of the objective function and constraint, initially minimizing drag with a constraint on the lift was found to be effective in producing converged designs. This procedure was also proven to be robust and efficient for cases where the drag varied smoothly, such as with the Euler solutions. The direct lift maximization with move limits which were fixed absolute values of the design variables, was also found to be a reliable and efficient procedure for designs based upon the Euler equations.

ACKNOWLEDGEMENT

REFERENCES

1. Volpe, G. and Melnik, R. M., "The Design of Transonic Airfoils by a Well-posed Inverse Method", *Int'L Journal for Numerical Methods in Engineering*, **22**, 1986, pp. 341–361.

2. Vanderplaats, G. N. and Hicks, R. M., "Numerical Airfoil Optimization Using a Reduced Number of Design Coordinates", NASA TM X–73151, July 1976.

3. Giles, M., Drela, M. and Tompkins, W. T. Jr., "Newton Solution of Direct and Inverse Transonic Euler Equations", AIAA Paper No. 85-1530, Jan. 1985.

Third International Conference on Inverse Design Concepts and Optimization in Engineering Sciences
(ICIDES-III). Editor: G.S. Dulikravich. Washington D.C., October 23-25, 1991.

4. Malone, J. B., Narramore, J. C. and Sankar, L. N., "An Efficient Airfoil Design Method Using the Navier-Stokes Equations", in *Computational Methods for Aerodynamic Design (Inverse) and Optimization*, AGARD CP-463, 1990, pp. 5.1-5.18.

5. Aidala, P. V., Davis, W. H. Jr. and Mason, W. H., "Smart Aerodynamic Optimization", AIAA Paper No. 83-1863, July 1983.

6. Vanderplaats, G. N., "Approximation Concepts for Numerical Airfoil Optimization", NASA TP 1370, 1979.

7. Joh, C.-Y., Grossman, B. and Haftka, R. T., "Efficient Optimization Procedures for Transonic Airfoil Design", proceedings ASME Winter Annual Meeting, AD-16, *Computational Structural Mechanics and Multidisciplinary Optimization*, editors: Grandhi, Stroud and Venkayya, Book No. H00534, Dec. 1989, pp. 67-76.

8. Joh, C.-Y., "Efficient and Robust Design Optimization of Transonic Airfoils", Ph.D. dissertation, Aerospace and Ocean Engineering, Virginia Polytechnic Inst. & State Univ., May 1991.

9. Grossman, B., Haftka, R. T., Kao, P.-J., Polen, D. M., Rais-Rohani, M. and Sobieszczanski-Sobieski, J. "Integrated Aerodynamic-Structural Design of a Transport Wing", *J. Aircraft*, 27, No. 12, 1990, pp. 1050-1056.

10. Schmit, L. A. and Farshi, B., "Some Approximation Concepts for Structural Synthesis", *AIAA J.*, 12, No. 7, 1974, pp. 692-699.

11. Grandhi, R.V., Thareja, R. and Haftka, R.T., "NEWSUMT-A: A General Purpose Program for Constrained Optimization using Constraint Approximations," *ASME Journal of Mechanisms, Transmissions and Automation in Design*, 107, 1985, pp. 94-99.

12. Spreiter, J. R., "Transonic Aerodynamics-History and Statement of the Problem", Chapter 1 in *Transonic Aerodynamics*, 81, Progress in Astronautics and Aeronautics, D. Nixon, Ed., AIAA, New York, 1982, pp. 3-66.

13. Murman, E. M., Bailey, F. R., and Johnson, M. H., "TSFOIL - A Computer Code for 2-D Transonic Calculations, Including Wind-Tunnel Wall Effects and Wave-Drag Evaluation", in NASA SP-347, Part II, 1975, pp. 769-788.

14. Jameson, A., Schmidt, W. and Turkel, E., "Numerical Solution of the Euler Equations by Finite Volume Methods Using Runge-Kutta Time Stepping Schemes", AIAA Paper No. 81-1259, June 1981.

15. Jameson, A., "Solution of the Euler Equations for Two Dimensional Transonic Flow by a Multi-grid Method", *Applied Mathematics and Computation*, 13, 1983, pp. 327-355.

16. Swanson, R. C. and Turkel, E., "A Multistage Time-Stepping Scheme for the Navier-Stokes Equations", AIAA Paper No. 85-0035, Jan. 1985.

17. Nixon, D., "Perturbation of a Discontinuous Transonic Flow", *AIAA Journal*, 16, No. 1, 1978, pp. 47-52.

18. Stahara, S. S., "A Rapid Approximation Procedure for Nonlinear Solutions: Application to Aerodynamic Flows and Design/Optimization Problems", Chapter 18 in *Transonic Aerodynamics*, 81, Progress in Astronautics and Aeronautics, D. Nixon, Ed., AIAA, New York, 1982.

change*	Lift Coeff.		Drag Coeff.		
%	Linear	Exact	Linear	Coord-St.	Exact
0.0		0.5341			0.00511
0.5	0.5472	0.5471	0.00584	0.00579	0.00585
-0.5	0.5210	0.5216	0.00439	0.00447	0.00436
1.0	0.5602	0.5614	0.00656	0.00654	0.00657
-1.0	0.5080	0.5098	0.00367	0.00396	0.00400
1.5	0.5733	0.5762	0.00728	0.00736	0.00755
-1.5	0.4949	0.4987	0.00295	0.00346	0.00342
2.0	0.5864	0.5918	0.00800	0.00827	0.00845
-2.0	0.4818	0.4881	0.00223	0.00302	0.00295

* Design variables increased by specified percentage from $(0.5, 0.5, -0.5, 0.5)^T$.

Table 1a. Lift and Drag Approximations - TSD.

change*	Lift Coeff.		Drag Coeff.		
%	Linear	Exact	Linear	Coord-St.	Exact
0.0		0.4878			0.00787
0.5	0.4948	0.4942	0.00866	0.00870	0.00854
-0.5	0.4809	0.4813	0.00708	0.00718	0.00724
1.0	0.5016	0.5006	0.00946	0.00957	0.00923
-1.0	0.4737	0.4749	0.00628	0.00652	0.00664
1.5	0.5086	0.5070	0.01029	0.01049	0.00996
-1.5	0.4667	0.4685	0.00549	0.00590	0.00607
2.0	0.5153	0.5135	0.01104	0.01149	0.01072
-2.0	0.4598	0.4621	0.00470	0.00533	0.00553

* Design variables increased by specified percentage from $(0.5, 0.5, -0.5, 0.5)^T$.

Table 1b. Lift and Drag Approximations - Euler.

Design cycle	Design Parameters				C_l	C_d	A
	X_1	X_2	X_3	X_4			
0	0.5	0.5	-0.5	0.5	0.5296	0.0059	0.0805
1	0.510	0.498	-0.524	0.490	0.4954	0.0040	0.0779
–	—	—	—	—	—	—	—
27	0.400	0.750	-0.649	0.481	0.5385	0.0040	0.0750
–	—	—	—	—	—	—	—
60	0.301	0.891	-0.763	0.565	0.5542	0.0040	0.0750
–	—	—	—	—	—	—	—
71	0.280	0.934	-0.805	0.591	0.5592	0.0040	0.0750

Table 2a. TSD Design Strategy A : Approximate Optimization with Tight Move Limits – initial condition 1.

Design cycle	Design Parameters				C_l	C_d	A
	X_1	X_2	X_3	X_4			
0	0.8	-0.4	0.7	-0.3	0.4418	0.0061	0.0739
1	0.837	-0.426	0.659	-0.281	0.4081	0.0038	0.0729
–	—	—	—	—	—	—	—
9	1.093	-0.483	0.504	-0.273	0.4061	0.0041	0.0750
–	—	—	—	—	—	—	—
11	1.114	-0.487	0.491	-0.275	0.4049	0.0040	0.0750
–	—	—	—	—	—	—	—
15	1.122	-0.487	0.487	-0.277	0.4055	0.0040	0.0750

Table 2b. TSD Design Strategy A : Approximate Optimization with Tight Move Limits – initial condition 2.

Design cycle	Design Parameters				C_l	C_d	A
	X_1	X_2	X_3	X_4			
0	1.0	0.0	0.0	0.0	0.5656	0.0103	0.0822
1	1.024	0.100	-0.075	-0.096	0.5195	0.0054	0.0750
2	0.773	0.280	-0.244	0.137	0.5041	0.0038	0.0750
3	0.631	0.417	-0.393	0.295	0.4999	0.0032	0.0750
4	0.504	0.516	-0.476	0.404	0.4989	0.0028	0.0750
5	0.418	0.650	-0.648	0.542	0.5005	0.0025	0.0750
6	0.071	1.038	-1.072	0.945	0.5080	0.0017	0.0750
7	0.080	1.308	-1.614	1.261	0.5124	0.0011	0.0750
8	0.001	1.475	-1.938	1.516	0.5049	0.0006	0.0750
*9	0.001	1.770	-1.863	1.215	0.6696	0.0034	0.0750
10	0.001	1.876	-1.940	1.209	0.7078	0.0041	0.0750

* begin lift maximization.

Table 3a. TSD Design Strategy B : Drag Minimization followed by Lift Maximization – initial condition 1.

case	Design Parameters				C_l	C_d	A	design cycles
	X_1	X_2	X_3	X_4				
1	1.0	0.0	0.0	0.0	0.5656	0.0103	0.0822	
	0.001	1.876	-1.940	1.209	0.7078	0.0041	0.0750	10
2	0.0	1.0	0.0	0.0	1.0676	0.0459	0.0771	
	-0.025	1.878	-1.889	1.179	0.7149	0.0042	0.0750	8
3	0.0	0.0	0.8	0.0	0.6491	0.0297	0.0786	
	0.043	1.904	-2.068	1.279	0.7034	0.0041	0.0750	13
4	0.0	0.0	0.0	1.0	0.5534	0.0242	0.0996	
	-0.006	1.923	-2.033	1.270	0.7091	0.0040	0.0750	10

Table 3b. TSD Design Strategy B : Drag Minimization followed by Lift Maximization – summary of designs with various initial conditions.

Design cycle	Design Parameters				C_l	C_d	A
	X_1	X_2	X_3	X_4			
0	1.0	0.0	0.0	0.0	0.5656	0.0103	0.0822
1	1.123	0.347	-0.491	0.041	0.5594	0.0061	0.0750
2	0.640	0.524	-0.452	0.263	0.5450	0.0043	0.0750
3	0.518	0.881	-0.844	0.473	0.5966	0.0045	0.0750
4	0.032	1.257	-1.000	0.737	0.6407	0.0044	0.0750
5	0.155	1.381	-1.249	0.785	0.6649	0.0046	0.0750
6	-0.006	1.524	-1.374	0.929	0.6672	0.0041	0.0750
7	-0.099	1.667	-1.504	1.024	0.6853	0.0041	0.0750
8	-0.224	1.916	-1.752	1.179	0.7218	0.0041	0.0750

Table 4a. TSD Design Strategy C : Approximate Optimization with Absolute Move Limits – initial condition 1.

case	Design Parameters				C_l	C_d	A	design cycles
	X_1	X_2	X_3	X_4				
1	1.0	0.0	0.0	0.0	0.5656	0.0103	0.0822	
	-0.224	1.916	-1.752	1.179	0.7218	0.0041	0.0750	8
2	0.0	1.0	0.0	0.0	1.0676	0.0459	0.0771	
	-0.332	2.035	-1.841	1.264	0.7360	0.0040	0.0750	8
3	0.0	0.0	0.8	0.0	0.6491	0.0297	0.0786	
	-0.539	2.340	-2.069	1.423	0.7922	0.0041	0.0753	8
4	0.0	0.0	0.0	1.0	0.5534	0.0242	0.0996	
	-0.434	2.077	-1.749	1.224	0.7638	0.0042	0.0750	5

Table 4b. TSD Design Strategy C : Approximate Optimization with Absolute Move limits – summary of designs with various initial conditions.

455

Third International Conference on Inverse Design Concepts and Optimization in Engineering Sciences
(ICIDES-III), Editor: G.S. Dulikravich, Washington D.C., October 23-25, 1991.

Move Limits	Design cycle	Design Parameters X_1	X_2	X_3	X_4	C_l	C_d	A	$C_{l_{equ}}$
	0	1.0	0.0	0.0	0.0	.48912	.011768	0.0810	
	1	0.827	0.100	0.094	-0.088	.49602	.009069	0.0750	
500%	2	0.555	0.331	-0.108	0.157	.49838	.007961	0.0750	
	3	0.325	0.558	-0.346	0.405	.49742	.006879	0.0750	
	4	-0.313	1.150	-0.923	1.040	.49438	.005745	0.0750	
	*5	-0.270	1.645	-1.231	0.927	.65665	.009951	0.0750	
	6	-0.375	1.924	-1.549	1.110	.68561	.009783	0.0750	
50%	7	-0.480	2.067	-1.665	1.200	.70255	.010024	0.0750	
	Δ8	-0.632	2.218	-1.777	1.319	.71358	.010223	0.0750	.70617
	9	-0.721	2.277	-1.822	1.390	.71068	.010204	0.0750	.70358
	10	-0.679	2.252	-1.822	1.375	.70759	.010026	0.0750	.70669
25%	Δ11	-0.729	2.303	-1.870	1.425	.70838	.010026	0.0750	.70746
	12	-0.792	2.350	-1.905	1.474	.70806	.010084	0.0750	.70484
12.5%	13	-0.729	2.295	-1.860	1.421	.70698	.010019	0.0750	.70660
	14	-0.721	2.302	-1.877	1.426	.70759	.009973	0.0750	.70864
	15	-0.717	2.307	-1.885	1.426	.70899	.009979	0.0750	.70980
	-	-	-	-	-	-	-	-	-
	22	-0.719	2.344	-1.931	1.446	.71384	.009999	0.0750	.71388
	23	-0.725	2.351	-1.939	1.452	.71404	.010001	0.0750	.71402
	24	-0.736	2.365	-1.954	1.465	.71427	.009998	0.0750	.71435
	25	-0.736	2.365	-1.953	1.465	.71439	.010002	0.0750	.71432

* begin lift maximization.
Δ starting point for reduced move limits.
** $C_{l_{equ}}$: Equivalent Value of C_l.

Table 5a. Euler Design Strategy B : Drag Minimization followed by Lift Maximization – initial condition 1.

Move Limits	Design cycle	Design Parameters X_1	X_2	X_3	X_4	C_l	C_d	A	$C_{l_{equ}}$
	0	1.0	0.0	0.0	0.0	.48912	.011768	0.0810	
	1	0.652	0.500	-0.220	0.057	.56529	.010919	0.0750	
	2	0.239	1.000	-0.672	0.455	.60127	.010031	0.0750	
	3	0.071	1.267	-0.923	0.634	.62789	.009978	0.0750	
0.5	4	-0.078	1.470	-1.098	0.772	.64813	.010042	0.0750	
	5	-0.227	1.635	-1.227	0.894	.66244	.010129	0.0750	
	6	-0.341	1.792	-1.380	1.018	.67371	.009992	0.0750	
	7	-0.434	1.956	-1.553	1.137	.68770	.009898	0.0750	
	8	-0.514	2.082	-1.675	1.226	.69950	.009951	0.0750	
	Δ9	-0.605	2.159	-1.722	1.288	.70507	.010117	0.0750	.70143
	10	-0.677	2.199	-1.749	1.342	.70144	.010089	0.0750	.69855
	11	-0.665	2.232	-1.805	1.362	.70542	.009989	0.0750	.70581
0.25	12	-0.721	2.292	-1.858	1.415	.70795	.010031	0.0750	.70684
	Δ13	-0.768	2.340	-1.907	1.465	.70768	.010012	0.0750	.70723
	14	-0.811	2.367	-1.924	1.495	.70710	.010064	0.0750	.70464
0.125	Δ15	-0.784	2.360	-1.931	1.486	.70734	.009989	0.0750	.70776
	16	-0.810	2.379	-1.942	1.504	.70790	.010040	0.0750	.70632
	17	-0.778	2.365	-1.942	1.488	.70809	.009970	0.0750	.70932
	-	-	-	-	-	-	-	-	-
0.02	29	-0.790	2.415	-2.005	1.521	.71310	.009997	0.0750	.71323
	-	-	-	-	-	-	-	-	-
	35	-0.804	2.435	-2.028	1.540	.71336	.009998	0.0750	.71345
	36	-0.807	2.438	-2.032	1.543	.71343	.010000	0.0750	.71339

Δ starting point for reduced move limits.
** $C_{l_{equ}}$: Equivalent Value of C_l.

Table 6a. Euler Design Strategy C : Approximate Optimization with Absolute Move Limits – initial condition 1.

case	Design Parameters X_1	X_2	X_3	X_4	C_l	C_d	A	design cycles
	1.0	0.0	0.0	0.0	0.4891	0.0118	0.0810	
1	-0.670	2.266	-1.837	1.371	0.7129	0.0101	0.0750	11
	0.0	1.0	0.0	0.0	0.6977	0.0266	0.0759	
2	-0.640	2.233	-1.801	1.337	0.7127	0.0101	0.0750	11
	0.0	0.0	1.0	0.0	0.5050	0.0467	0.0967	
3	-0.649	2.237	-1.803	1.344	0.7121	0.0101	0.0750	12
	0.0	0.0	0.0	1.0	0.3558	0.0165	0.0984	
4	-0.630	2.206	-1.772	1.322	0.7090	0.0101	0.0750	10

Table 5b. Euler Design Strategy B : Drag Minimization followed by Lift maximiation – summary of designs with various initial conditions.

case	Design Parameters X_1	X_2	X_3	X_4	C_l	C_d	A	design cycles
	1.0	0.0	0.0	0.0	0.4891	0.0118	0.0810	
1	-0.605	2.159	-1.722	1.288	0.7051	0.0101	0.0750	9
	0.0	1.0	0.0	0.0	0.6977	0.0266	0.0759	
2	-0.636	2.194	-1.759	0.323	0.7055	0.0101	0.0750	8
	0.0	0.0	1.0	0.0	0.5050	0.0467	0.0967	
3	-0.650	2.208	-1.774	1.339	0.7049	0.0100	0.0750	10
	0.0	0.0	0.0	1.0	0.3558	0.0165	0.0984	
4	-0.664	2.255	-1.833	1.372	0.7090	0.0101	0.0750	9

Table 6b. Euler Design Strategy C : Approximate Optimization with Absolute Move limits – summary of designs with various initial conditions.

Airfoils	$C_l/C_{d_{wave}}$ TSD Anaysis	Euler Analysis
Airfoil 1	54.9	41.4
Airfoil 2	23.3	26.2
Airfoil 3	21.9	23.9
Airfoil 4	22.9	21.6
Optimized, TSD	171.0	83.4

Table 7. Error Maginification during Optimization.

...... Base solution, X = (0.50, 0.50,-0.50, 0.50)
o-o Approximation, X = (0.51, 0.51,-0.49, 0.51)
—— Exact Analysis, X = (0.51, 0.51,-0.49, 0.51)
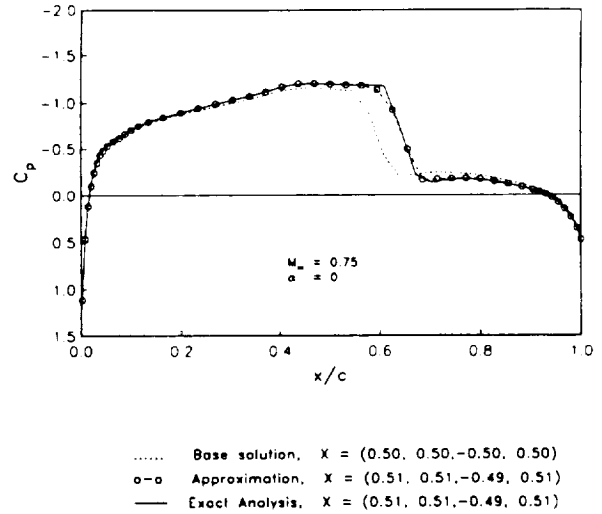
Figure 1a. Approximation of Pressure Distribution Based On the Method of Strained Coordinates – TSD.

...... Base solution. X = (0.50, 0.50,-0.50, 0.50)

o-o Approximation. X = (0.51, 0.51,-0.49, 0.51)

——— Exact Analysis. X = (0.51, 0.51,-0.49, 0.51)
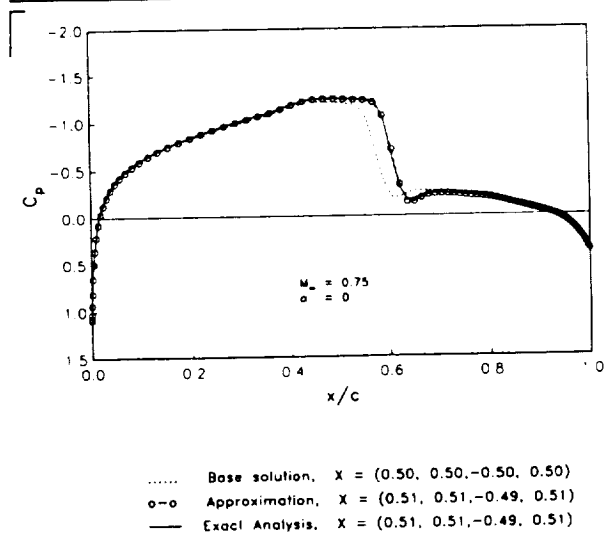
Figure 1b. Approximation of Pressure Distribution Based On
the Method of Strained Coordinates - Euler.

—o— Exact Value

--•-- Approximate Value
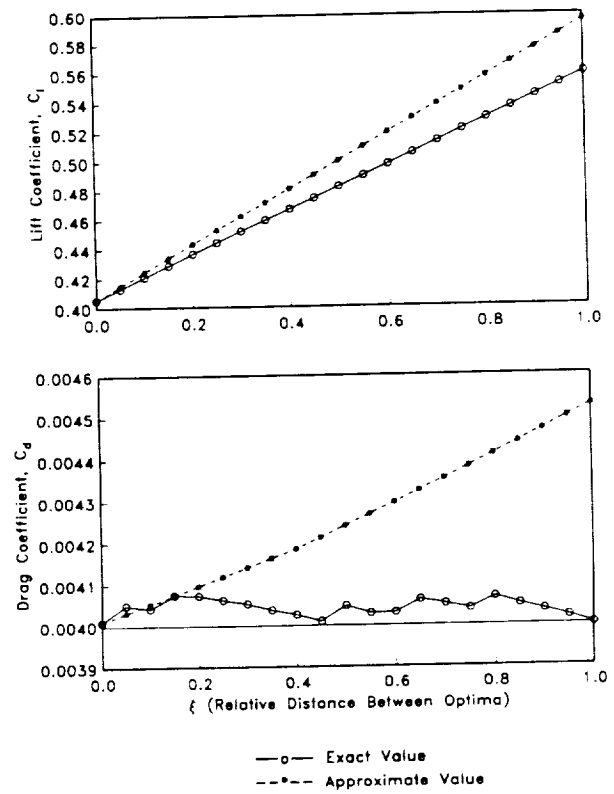
Figure 2. Objective Function and Constraint
Behavior for Two TSD Local Optima.

.... Initial Design
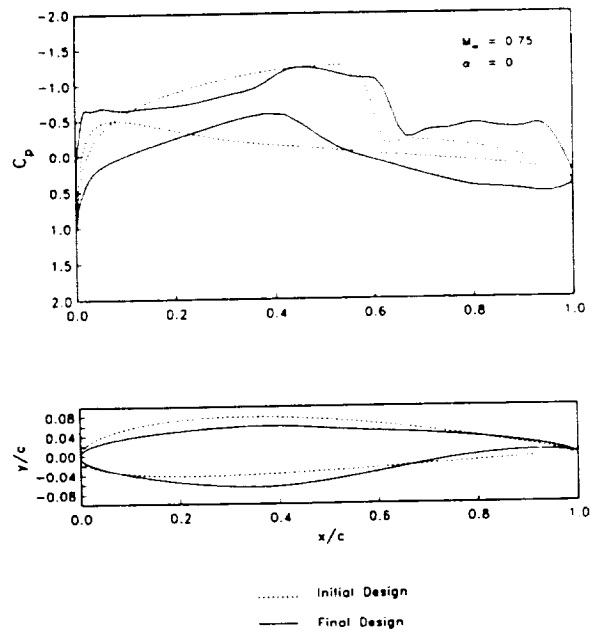
——— Final Design
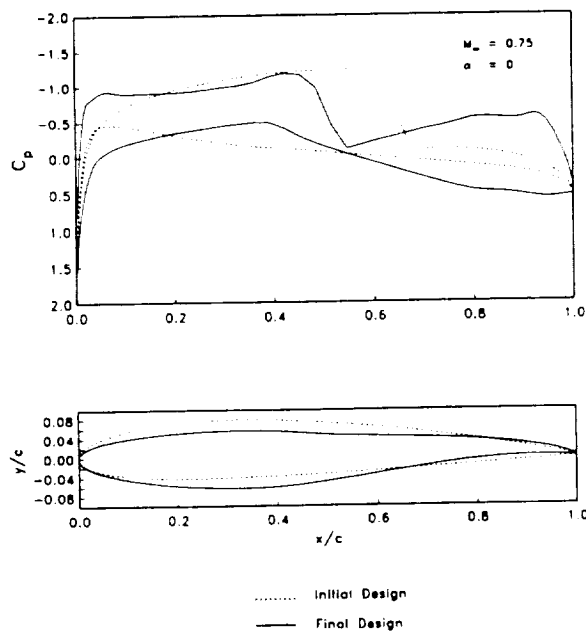
Figure 3. TSD Design Results

.... Initial Design

——— Final Design

Figure 4. Euler Design Results